

# Effects of Roadway Geometric Features on Low-Speed Turning Maneuvers of Large Vehicles

Juey-Fu Cheng<sup>1+</sup>, and Hsuan-Chih Huang<sup>1</sup>

**Abstract:** Vehicle turning maneuver is a major design control in roadway alignment, pavement and the placement of curbs at highway intersections. Geometric features, such as the sharper curvature at turning roadways have significant effects on turning maneuverability of vehicles. Due to their wider and longer wheelbases, large vehicles have much more pronounced offtracking and occupy greater swept-path widths. This often creates complex driving operations when large vehicles turn at intersections. The turning maneuvers of large vehicles not only determine roadway design, but also influence the safety and efficiency of intersection operations. Studying turning maneuvers mainly consists of analyzing vehicle turning paths and steering operations. This study presents a computational approach that can simulate vehicle turning maneuverability for given roadway alignments, and also checks for coincidence with design standards. This study also presents field experiments involving tractor-semitrailer truck and bus on roadways with different geometric features. The turning paths of wheels and steering wheel operations were recorded simultaneously. Data from field experiments of different turning angles and roadway geometric features are compared with simulated results of computational approach. This study also analyzes the effects of curve radius and geometric features on turning maneuvers. The precise analysis of vehicle turning maneuvers, including turning paths, swept widths, and steering operations, could help roadway and pavement engineers improve traffic safety and efficiency.

**Key words:** *Offtracking; Steering operation; Vehicle turning path.*

## Introduction

Highway intersections create through, crossing, and turning movements for vehicles and therefore contain a number of traffic conflict points. Low-speed turning maneuverability of vehicles is a major consideration in the design of intersections and turning roadways. To serve turning movements between approach legs, the design of turning roadways should be based on vehicle turning maneuvers, which mainly involve vehicle turning paths and steering operations. Vehicle turning paths affect horizontal alignment design, lane widening, and the placement of curbs for turning roadways, while steering operations influence the smoothness and efficiency of driving.

Traffic in Taiwan consists of a mixture of large vehicles, cars, and a considerable number of motorcycles. Intersections contain points of conflict between vehicles, bicycles and pedestrians. Large vehicles are a threat to motorcyclists and pedestrians, particularly at intersections in industrial and harbor areas. The design of turning roadways should therefore endeavor to mitigate the effects of large vehicles on the safety of smaller and more vulnerable vehicles. Studying and clarifying the effects of roadway geometric features on large vehicles' turning maneuvers could help traffic engineers plan the layout of intersections, the movement paths of different traffic flows, and the design of signal phasing.

Offtracking occurs when a vehicle makes a turn and its rear wheels do not follow the same path as its front wheels. While there are two types of offtracking, low-speed offtracking and high-speed

offtracking. The intersection design usually focuses on low-speed conditions. As a vehicle negotiates a turn at low speed, offtracking occurs when the rear wheels track inside the front wheels. Even when the turning roadway alignment is a simple circular curve, the tracks of the inner rear wheels do not follow circular or spiral curves as a result of off-tracking behavior. The configuration of a vehicle turning path depends on roadway alignment and the type and dimensions of the vehicle: vehicles with wider and longer wheelbases have much more pronounced offtracking and occupy greater swept-path widths.

Complex driving operations may arise when large vehicles turn at intersections. Rapid and significant changes in the steering angle can create difficulty for the driver. A combination vehicle has more articulation points and more wheelbases (i.e., distances between axles). The combination vehicle driver must perform steering operations while paying attention to the deflection of the vehicle body.

Highway design standards require roadway widening on horizontal curves to accommodate the greater width of some large vehicles. The amount of widening depends on vehicles dimensions and roadway curvature. Taiwanese design specification [1] provides dimensions for six types of design vehicles. The AASHTO Green Book [2] establishes nineteen design vehicles in four general classes (passenger cars, buses, trucks, and recreational vehicles).

Because turning roadways at intersections typically have a lower design speed, the configuration of vehicle turning paths is as important as widening. The highway design standards mentioned above present the minimum turning paths for all the design vehicles. Highway engineers can combine these templates with their own designs to check for the adequacy and coincidence of roadway geometry. However, the minimum turning paths might not be enough for engineering applications when (1) roadway alignments are other than simple circular curves, (2) roadway alignments have a

<sup>1</sup> Department of Civil and Ecological Engineering, I-Shou University, Taiwan.

<sup>+</sup> Corresponding Author: E-mail chengjf@isu.edu.tw

Note: Submitted July 25, 2010; Revised January 11, 2011; Accepted March 2, 2011.

radius greater than the minimum, or (3) turns are other than the specific angles.

In the geometric design of turning roadways, the analysis of vehicle turning paths and swept widths can help identify conflict areas of different traffic movements or potential collision points at curbs and determine the pavement configuration of turning lanes coincident with vehicle turning paths. This in turn can help improve roadway design and safety at intersections. Further study on driving maneuvers corresponding to roadway alignment, including steering and articulation angles and their changing rates, could be used to analyze and improve the smoothness of driving operations, and thus increase the efficiency of intersections.

## Literature Review

Offtracking is the difference between the paths of front and rear wheels [2, 3]. It generally increases with the spacing between the axles of the vehicle and decreases for larger radius turns. The swept-path width can be calculated from the total offtracking and the width of the vehicle. The traditional method, known as the "sum of the squares," can predict steady-state (maximum) offtracking [4, 5]. The Western Highway Institute (WHI) simplified this method from the earlier work of the Society of Automotive Engineers (SAE).

Transient offtracking describes turning paths before maximum offtracking is reached. Compared to mathematical offtracking formulas, a computer simulation has the advantage of providing both steady-state offtracking and transient offtracking estimates. In the 1980s, The University of Michigan Transportation Research Institute (UMTRI) produced the first vehicle offtracking model for the Federal Highways Administration (FHWA) [6]. Caltrans [7, 8] and FHWA [9] began to develop computer programs for analyzing and evaluating truck offtracking that outperformed an earlier graphic instrument known as a Tractrix Integrator. From the 1990s onward, commercial add-on programs configured on CADD software (such as AutoCAD and Microstation) have enabled users to model vehicular swept paths and check the design of intersections. These programs include Transoft Solutions' AutoTURN [10, 11] and Savoy Computing Services' AutoTrack [12]. AutoTURN also has the ability to generate and revise vehicle turning path templates.

Turning paths may also be analyzed by formulating and solving equations of a given vehicle's motion. Freedman and Riemenschneider [13] derived a differential equation to describe path of the rear wheels for a bus whose front axle travels on a smooth path. The solution to this equation describes the motion of a bus turning or changing lanes. Alexander and Maddocks [14] discussed kinematics and derived equations to govern the motion of rolling vehicles. They then used the equations to describe the offtracking of vehicles while turning. Wang and Linnett [15] developed a mathematical model for computing the path of any point on wheeled vehicles. This model makes it possible to analyze the independence of the vehicle's orientation angle, steering angle, and curvature. Prince and Dubois [16] proved that the path of the rear wheels is independent of speed, assuming that the wheels are not slipping. They introduced ordinary differential equations and solutions for the rear wheels of a bus, cab-trailer, and articulated truck. Other researchers proposed the driving hazard problem of a

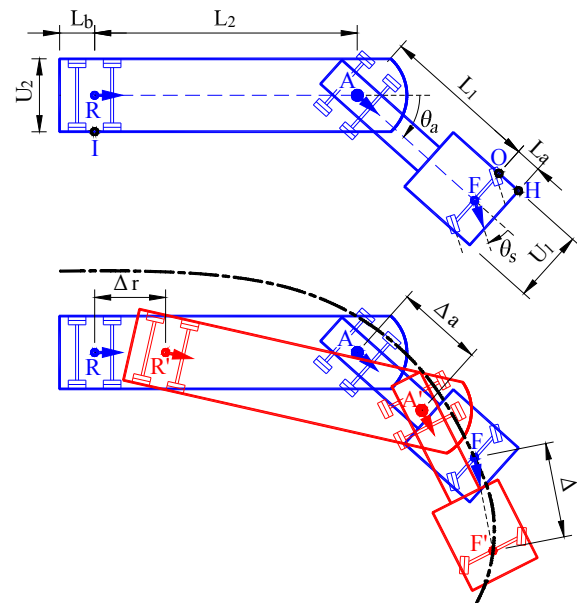


**Fig. 1.** Vehicle Dimensions and Turning Tendency.

vehicle making a right turn with the rear (overhang) of the vehicle swinging leftward toward an unsuspecting driver passing on the left. Wang and Cai investigated the mathematical models for this problem and the simulation of turning motions [17].

The most accurate and reliable, though time-consuming, method of obtaining a vehicle turning path is by a full-scale field test. The actual wheel paths can be marked and/or measured on site, although field tests are restricted to available vehicles with different dimensions and configurations. SAE set forth a field-test procedure to determine the maximum offtracking and minimum turning diameter of motor vehicles [4]. The paths can be marked on the pavement by pouring water on the tires while the wheels are turned to the maximum cut angle while making complete circle turns. Gattis and Howard [18] conducted a field test to determine the turning radii and swept paths of selected school buses. They used burettes attached to the bus body and an apparatus that sprayed water on the tires to mark the bus paths during the sharpest possible turns. Terry and Schuster [19] investigated the variables affecting the turning path of a reversing tractor-trailer, and used chalk to mark the reverse movement paths. Transoft Solutions also conducted field tests for vehicle driving paths with GPS receivers mounted on the top of vehicles to record the location of front and rear axles.

## Computational Approach

This study presents a simplified computational approach for engineering applications. This iterative numerical method may be used to calculate low-speed vehicle turning paths and their corresponding steering and articulating angles. The following are the basic assumptions and computation procedure for the example of tractor-semitrailer combination truck (Fig. 1).

### Basic Assumptions

- There is no slip angle on any of the tires. Furthermore, the orientation of instant velocity for every axle is assumed to be

the same as the orientation of the wheels, as the arrows show on points F, A, and R (Fig. 1).

- The vehicle dimensions are known, including vehicle widths ( $U_1, U_2$ ), effective vehicle wheelbases ( $L_1, L_2$ ), front and rear overhangs ( $L_a, L_b$ ), and location of the articulation point.
- The initial status of the vehicle, including the center points of each axle group (F, A, R), is given.
- The center point of the front axle (F) follows a given roadway alignment.

**Computation Procedure**

- 1) Calculate direction vectors  $\overline{AF}$  and  $\overline{RA}$ .
- 2) Calculate the positions of outer front wheel (O) and outer front overhang (H) from F using  $\overline{AF}$  and vehicle dimensions  $U_1$  and  $L_a$ .
- 3) Calculate the position of inner rear wheel (I) from R using  $\overline{RA}$  and vehicle dimension  $U_2$ .
- 4) Turn the front wheels to the direction from F to  $F'$ , and move the center point of the front axle forward by a small displacement ( $\Delta$ ) following the given roadway alignment.
- 5) Calculate the movement vector  $\overline{FF'}$ .
- 6) Calculate the steering angle  $\theta_s$  and articulating angle  $\theta_a$  :

$$\theta_s = \overline{FF'} - \overline{AF} \tag{1}$$

$$\theta_a = \overline{AF} - \overline{RA} \tag{2}$$

- 7) Calculate the displacements of the articulation point ( $\Delta_a$ ) and the center point of the rear axle ( $\Delta_r$ ):

$$\Delta_a = L_1 + \Delta \cdot \cos\theta_s - [L_1^2 - (\Delta \cdot \sin\theta_s)^2]^{1/2} \tag{3}$$

$$\Delta_r = L_2 + \Delta_a \cdot \cos\theta_a - [L_2^2 - (\Delta_a \cdot \sin\theta_a)^2]^{1/2} \tag{4}$$

- 8) Find the new position of the articulation point ( $A'$ ) using direction vector  $\overline{AF}$  and displacement  $\Delta_a$ .
- 9) Find the new position of the center point of the rear axle ( $R'$ ) using direction vector  $\overline{RA}$  and displacement  $\Delta_r$ .
- 10) Return to Step 1 and repeat Steps 1 through 9 until the entire vehicle turning path is established.

Assuming that the outer front wheel, instead of center point of the front axle, follows a given roadway alignment, a similar computation procedure can be used to calculate the vehicle's turning path. In this case, the new position of the articulation point ( $A'$ ) should be determined in advance, using direction vector  $\overline{AF}$  and vehicle dimensions  $U_1$  and  $L_1$ , after each iterative movement. It is then possible to calculate the position of the center point of the front axle ( $F'$ ).

**Computer Program**

This study develops a computer program to calculate a vehicle turning path that follows a given roadway alignment. The roadway alignment could be any continuous horizontal alignment, and not just a simple circular curve.

One of the important parameters for the computation procedure mentioned above is the iterative displacement step ( $\Delta$ ). Parameter

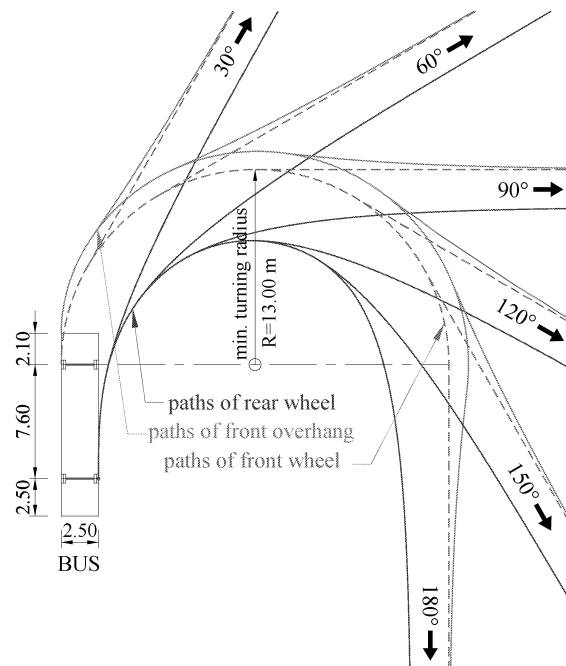


**Fig. 2.** Minimum Turning Paths of BUS.

calibration shows that as the step decreases, the configuration of a vehicle turning path can converge rapidly. Consider the example of the minimum turning path of an AASHTO intermediate semitrailer truck WB-15. When  $\Delta$  varies from 1.0 m to 0.01 m, there are no significant differences for the paths of the outer front wheel and overhang, but the maximum difference of paths of the inner rear wheel would be about 52 cm. For general applications in engineering analysis and design, an iterative step of 0.1 m is sufficient to obtain reasonable precision, and the above-mentioned difference can be less than 5 cm compared to convergent state.

**Program Verification**

To confirm the practical applicability of this procedure, design vehicles defined by Taiwan and AASHTO highway design standards [1, 2] were selected to simulate the minimum turning paths, and the corresponding exhibits in these design standards were then overlapped to check for consistency. The calculated paths match the figures contained in the design standards. Figs. 2 and 3 present the calculated minimum turning paths of BUS [1] and WB-15 [2].

**Steering and Articulating Angles**

The maximum steering angle of the vehicle imposes a limit on its minimum turning radius. Fig. 4 and 5 demonstrate the calculated steering and articulating angles corresponding to minimum turning paths of BUS and WB-15. The steering angle of BUS increases rapidly when it initially enters the circular turning roadway, and then the rate of increase gradually slows down as the turning continues. The maximum steering angle ( $38.8^\circ$ ) appears at the end of the circular curve, and then decreases sharply immediately after entering the tangent section. The steering angle of WB-15 has a similar curve shape, but it reaches a stable maximum value of  $17.8^\circ$

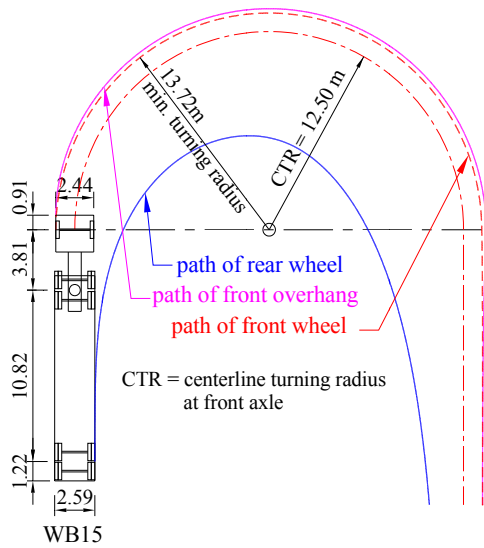


Fig. 3. Minimum Turning Paths of WB-15.

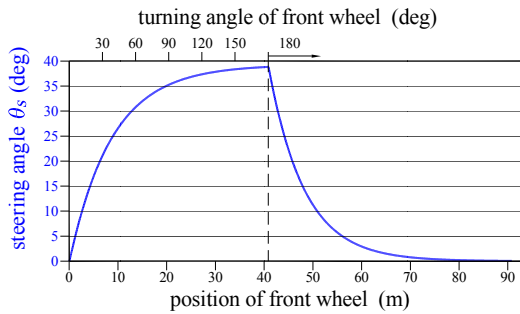


Fig. 4. Steering Angle of Minimum Turning Paths of BUS.

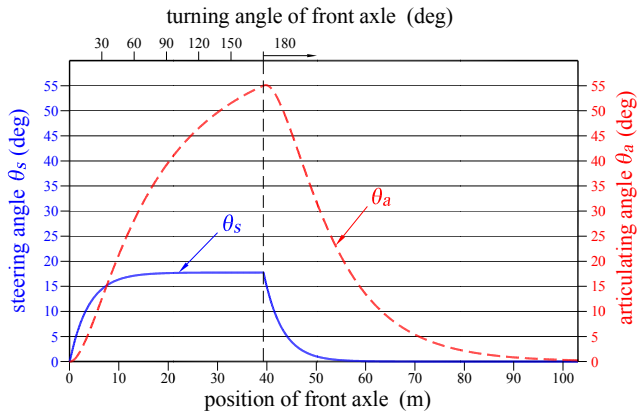


Fig. 5. Steering and Articulating Angle of Minimum Turning Paths of WB-15.

from a vehicle turning angle of about 90°. The articulating angle of WB-15 has a greater maximum value of 55.2°.

## Field Experiment

### Test Vehicles

A field experiment investigating vehicle turning paths was undertaken with the objective of confirming the accuracy of the

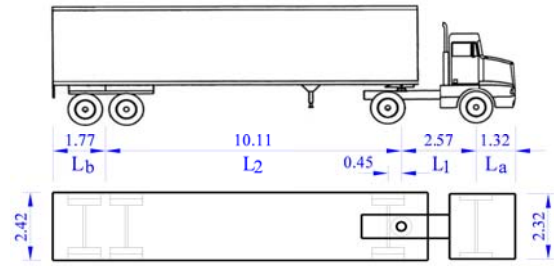


Fig. 6. Dimensions of Test Vehicle (Tractor-semitrailer).

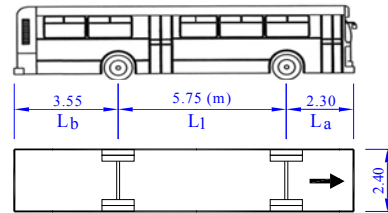


Fig. 7. Dimensions of Test Vehicle (Bus).

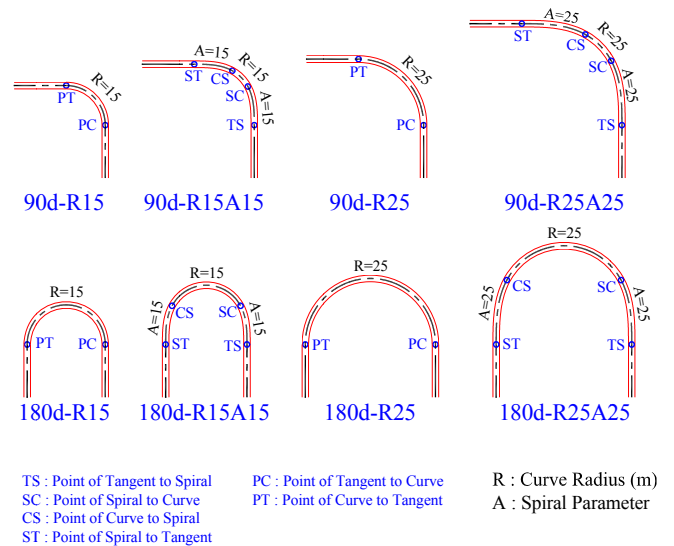


Fig. 8. Turning Roadways of Field Experiment.

computational approach and effects of geometric features. Two test vehicles, a tractor-semitrailer truck and a bus, were used to represent combination vehicles and single-unit vehicles, respectively. Fig. 6 and 7 illustrate the dimensions of the test vehicles.

### Experiment Roadway

Geometric factors of the field experiment include turning angle, radius, and transition (spiral) curve. Fig. 8 shows the left turn roadways of the field experiment. The eight roadways used in the experiment vary with regard to two turning angles (90° and 180°), two circular radii (15 and 25 m), and whether they have or do not have spiral transitions. The roadway code below every graph states its geometric properties. The tractor-semitrailer had carried out all the experiment of 90° and 180° turning roadways, but the bus just carried out the experiment of 90° turning roadways due to limitation of site work.



Fig. 9. Site Preparation Work.

### Site Preparation

The centerline of every experimental roadway alignment was set up on site precisely (Fig. 9). The beginning and end points of each roadway alignment, and all connection points of roadway elements (tangent sections, circular curves, spiral transitions), were first located using an electronic theodolite according to their coordinates. To form the complete alignment configuration, points along the centerline were marked by a deflection angle surveying method with a constant interval of 1 m.

Symmetrical parallel lines on both sides of the roadway centerline were drawn based on the width of the test vehicle to guide the driver of the experiment. Cross-lines perpendicular to the centerline were also drawn with the same constant interval of 1 m, and a graduation of cross-lines was regularly marked to determine the swept path of the vehicle.

### Data Collection

When the field experiment was undertaken, a test vehicle was driven along the turning roadway at a low speed of 5-10 km/hr. Video recorders were operated manually beside all wheels of the test vehicle to record the swept paths. Another video recorder was placed behind the driver to record the operation of the steering wheel. All recorded video was synchronized by whistle signals whenever the test vehicle passed a critical experiment roadway point (e.g., TS, SC, CS, ST, etc.). The field experiment for every turning roadway was executed twice, and the experiment exhibiting the best agreement between the front-wheel path and roadway alignment was chosen for analysis.

Video editing software was used to extract images from recorded video files of swept paths and the steering wheel in a time sequence. The resulting series of images was interpreted by computer. The precise interpolation positions of swept paths were measured using a computer ruler, and the angles of the steering wheel were measured using a computer protractor.

Field observation indicated that, to follow the roadway alignment in the experiment, the drivers often swung the steering wheel left and right repeatedly within a certain range. The original angle data of the steering wheel measured from video also shows random higher-frequency fluctuations. A multiple-pass moving average filter [20] was used to remove noise from the angle data of steering wheel and reveal the effects of turning roadway alignment on the operation

of the steering wheel.

## Experiment Results and Discussion

Measured data of different turning angles and roadway geometric features from the field experiment were all redrawn in AutoCAD, and then the vehicle turning paths and steering operation were analyzed and compared with the simulated results of the computational approach. According to recorded video of all wheels of the test vehicles, the paths of the outer front wheel and the inner rear wheel determined the configuration of the vehicle turning path. The path of the outer front overhang was not recorded.

The tractor-semitrailer from roadways 180d-R15 and 180d-R15A15 were used to demonstrate the field experiment results. Fig. 10(a) and 10(b) respectively illustrate the 180d-R15 and 180d-R15A15 turning paths of each tractor-semitrailer, including those measured in the field test and simulated by the computational approach. The measured paths of the outer front wheel could closely meet the simulated paths (Fig. 10). The measured paths of the inner rear wheel are inside the simulated paths. The paths of the inner rear wheels are not symmetrical, and the positions of maximum swept-path width appear at later sections of the turning roadways.

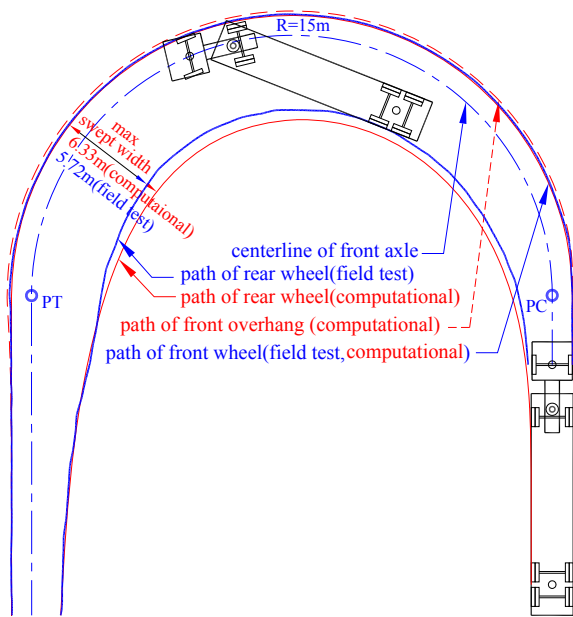
Fig. 11(a) and 11(b) show the swept-path widths of the tractor-semitrailer on roadways 180d-R15 and 180d-R15A15, respectively. The measured path widths are generally smaller than simulated path widths. The maximum swept path widths of 180d-R15 and 180d-R15A15 measured from field experiment are 5.72 m and 5.62 m, they are smaller than simulated results by about 61-63 cm. The positions where the maximum swept-path width appears are almost the same in measured and simulated results.

The maximum swept-path width of roadway 180d-R15A15 (with spiral transitions) is slightly less than the roadway 180d-R15 (without spiral transitions). However, this difference cannot solely be attributed to the effect of spiral transition because the lengths of the turning roadways from tangent to tangent are also different.

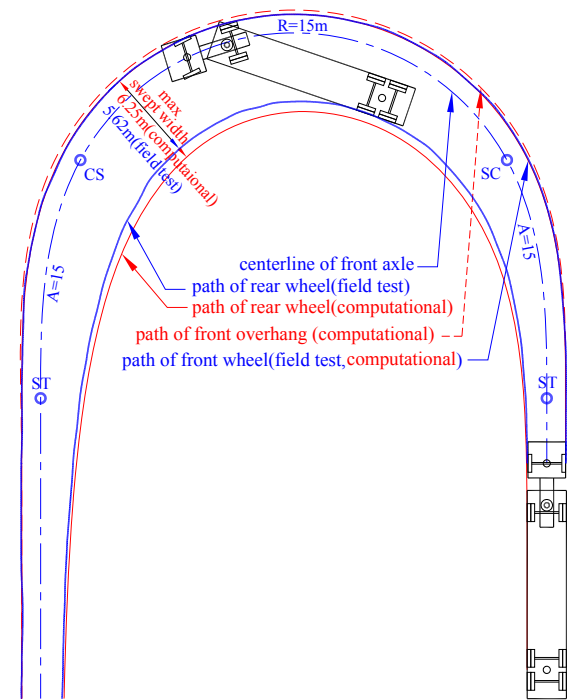
The steering ratio [21] refers to the ratio between the turning angle of the steering wheel and the deflection angle of the front wheels (i.e. steering angle). Assuming that the steering ratio of a vehicle remains constant, the degree of the steering angle relates directly to the turning angle of the steering wheel, and the changing rate of the steering angle relates to the angular speed of the steering wheel. These data can be used to analyze the steering or driving operations of the vehicle.

Fig. 12(a) and 12(b) show the angle of the steering wheel measured in the field experiment and the simulated steering and articulating angles of the tractor-semitrailer on roadways 180d-R15 and 180d-R15A15, respectively. Because all turning roadways in the experiment were left turns, all angle values shown in the figures are negative. The angle of the steering wheel (measured) and steering/articulating angle (simulated) appear on different vertical axes scale in Fig. 12. The ratio of the two vertical axes scales is 25, which implies the steering ratio of the tractor-semitrailer, and could therefore link the angle of the steering wheel and the steering angle (deflection angle of the front wheel).

The computational curves  $\theta_s$  in Fig. 12 illustrate the corresponding steering angles when the test vehicle follows the



(a) 180d-R15

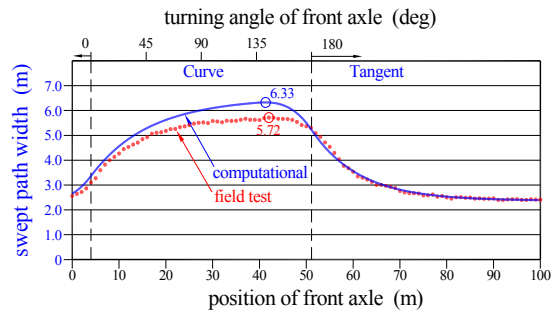


(b) 180d-R15A15

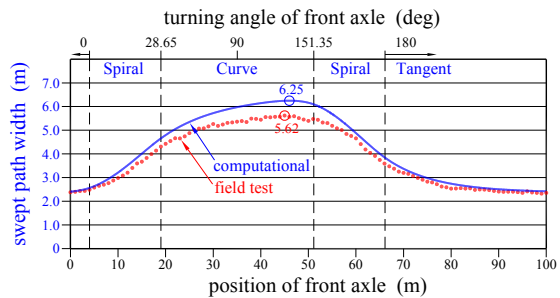
**Fig. 10.** Turning Paths of Tractor-semitrailer.

experimental roadway alignments exactly. Both the  $\theta_s$  curves in Fig. 12(a) and 12(b) yield the same stable maximum value of  $-9.87^\circ$  after entering the circular curve for a distance.

The measured angles of the steering wheel, after filtering the repeated swinging motion, are shown as curves  $\theta_w$  in Fig. 12(a) and 12(b). The tendency of curves  $\theta_w$  is similar to that of curves  $\theta_s$ , even though there are still some observable fluctuations on the curves  $\theta_w$  due to the driver's effort to follow the roadway alignments precisely. However, the curve  $\theta_w$  of the experimental roadway with spiral transitions (180d-R15A15) is more coincident with the curve  $\theta_s$ , especially at the entering and leaving sections of

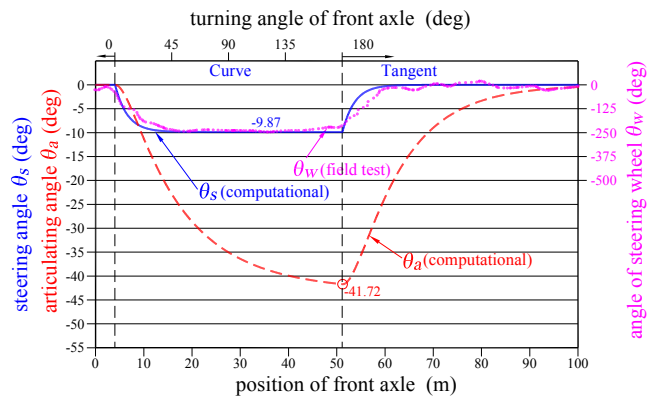


(a) 180d-R15

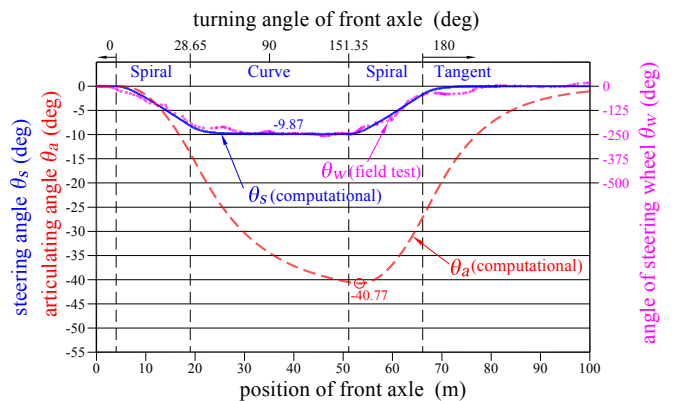


(b) 180d-R15A15

**Fig. 11.** Swept Path Width of Tractor-semitrailer.



(a) 180d-R15



(b) 180d-R15A15

**Fig. 12.** Steering and Articulating Angle of Tractor-semitrailer.

the turns. This could indicate that the turning roadway with transition sections is easier for drivers to follow.

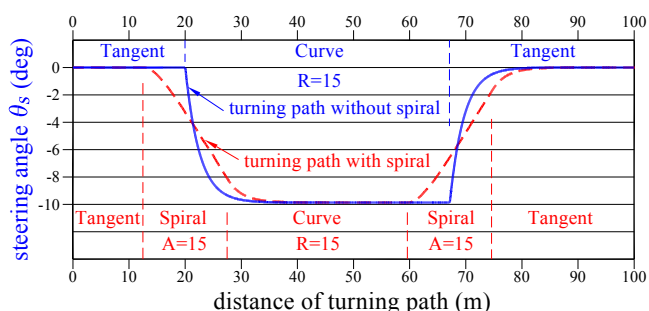


Fig. 13. Effect of Spiral Transition on Steering Angle.

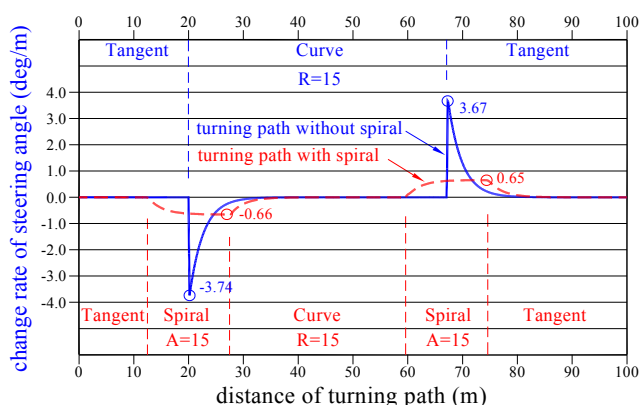


Fig. 14. Effect of Spiral Transition on Steering Angle Changing Rate.

Fig. 12(a) and 12(b) also show the simulated articulating angles with and without spiral transitions. The maximum values of the articulating angles for 180d-R15 and 80d-R15A15 are  $-41.72^\circ$  and  $-40.77^\circ$ , respectively. The maximum articulating angle of experimental roadway with spiral transitions is slightly smaller, and

the changing rates (slopes of the curve) at entering and leaving sections of the turns are also milder.

The simulated steering angles of the tractor-semitrailer of 180d-R15 and 180d-R15A15 overlap at the midpoint of turning roadways in Fig. 13. In the case of 180d-R15A15, most of the increasing and decreasing of steering angles occurred over a certain distance on the spiral transitions. However, the steering angles of 180d-R15 change rapidly after the beginning and end points of turning roadway. Fig. 14 shows the changing rates of steering angles. The peak clockwise and counterclockwise steering angle changing rates significantly decreased from 3.67 and  $-3.74 \text{ deg/m}$  to 0.65 and  $-0.66 \text{ deg/m}$  in the presence of spiral transitions. Field experiments also indicate that a roadway without spiral transitions makes it harder for drivers to follow the entering and leaving sections, causing the driving path to deviate a little from the preset alignment.

Table 1 shows important data of all experimental roadways. All the measured results of maximum swept-path widths are smaller than the simulated results by the range of 29 to 63 cm for the tractor-semitrailer, while there is no significant difference for the bus on  $90^\circ$  turns. The reason for this difference could be the effect of slip angle on tires. The influence of slip angle on a combination vehicle is more significant due to deflection of the vehicle body.

When the radius of experimental roadways increases from 15 m to 25 m, the measured maximum swept-path widths decrease significantly, especially at  $180^\circ$  turning roadways with the tractor-semitrailer which have decreasing rates of 21-23%. The existence of spiral transitions has little effect on maximum swept-path width, maximum steering angle, and maximum articulating angle. On the other hand, spiral transitions can greatly help to decrease maximum changing rates for steering angles; the decreasing range for the tractor-semitrailer is 82-89%, and 63-77% for the bus.

Table 1. Results of Field Experiment and Computational Approach.

Roadway	Max. Swept Path Width (m)			Max. $\theta_s$ (deg)	Max. $\theta_a$ (deg)	Rate. $+\theta_s$ (deg/m)	Rate. $-\theta_s$ (deg/m)
	Field	Comput.	$\epsilon$				
<b>Tractor-Semitrailer</b>							
90d-R15	5.11	5.57	-0.46	-9.86	-35.22	3.69	-3.75
90d-R15A15	4.93	5.33	-0.4	-9.81	-31.52	0.67	-0.66
90d-R25	4.18	4.51	-0.33	-5.9	-23.15	2.23	-2.25
90d-R25A25	4.08	4.37	-0.29	-5.91	-21.49	0.24	-0.26
180d-R15	5.72	6.33	-0.61	-9.87	-41.72	3.67	-3.74
180d-R15A15	5.62	6.25	-0.63	-9.87	-40.77	0.65	-0.66
180d-R25	4.25	4.62	-0.37	-5.9	-23.96	2.2	-2.25
180d-R25A25	4.3	4.61	-0.31	-5.92	-23.9	0.24	-0.26
<b>Bus</b>							
90d-R15	3.35	3.41	-0.06	-22.07	-	3.69	-3.79
90d-R15A15	3.27	3.35	-0.08	-20.69	-	1.35	-1.36
90d-R25	3.04	3.02	0.02	-13.28	-	2.26	-2.27
90d-R25A25	3	3.01	-0.01	-13.05	-	0.52	-0.55

Max. $\theta_s$ : maximum steering angle (computational)

Max. $\theta_a$ : maximum articulating angle (computational)

Rate. $+\theta_s$ : maximum clockwise steering angle changing rate (computational)

Rate. $-\theta_s$ : maximum counterclockwise steering angle changing rate (computational)

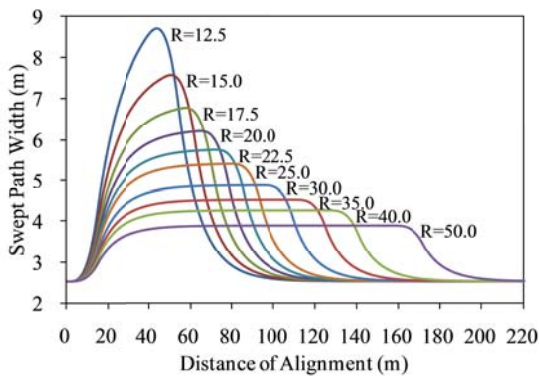


Fig. 15. Swept Path Widths of Different Radius Roadways.

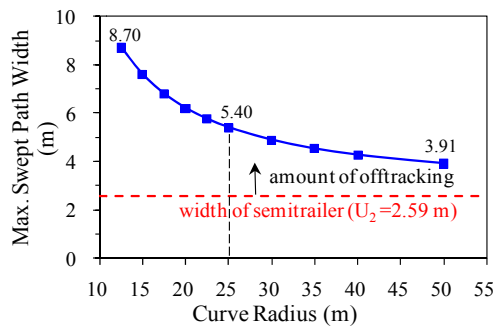


Fig. 16. Effect of Curve Radius on Max. Swept Path Width.

Field experiments were conducted on a wharf site instead of real turning roadways. The front axle of test vehicles was required to closely follow the preset roadway alignments at low speed, ignoring car-following behavior in traffic flow. The vehicle speed of intersection turning roadways usually remains within the range of low speed offtracking, and a slightly higher speed could result in smaller swept width. Under realistic traffic conditions, experienced drivers may shift their driving paths slightly off the roadway alignment to reduce the effect on driving operations or swept widths. Disregarding illegal driving behavior, results of the field experiment should be conservative from the engineering design viewpoint.

### Effects of Curve Radius

Due to the limitations of the experimental environment, more experiments on roadway alignments with different curve radii could not be conducted. To examine the effects of curve radius on turning maneuverability, this study employs the intermediate semitrailer truck WB-15, which is defined by AASHTO (all dimensions in Fig. 3), to simulate turning paths with different curve radii using the computational approach.

The simulated roadway alignments consist of circular curve and tangent sections with 180° turning angles. These sections have the same composition as 180d-R15, but involve right turns. The curve radius of simulated roadways varies from 12.5 m to 50 m, with a total of 10 alignments. A radius greater than 50m could result in a higher travel speed, and the analysis of low-speed turning maneuvers may not be applicable.

### Swept-Path Width

Fig. 15 shows the curves of swept-path width for roadways with different radii. The width of the swept path changes rapidly at the entering and leaving sections. This figure also shows that the roadways have greater radii, which given longer turning roadways, could create a stable maximum swept-path width.

Fig. 16 shows the relationship between the curve radius and simulated maximum swept-path width (including front overhang) for WB-15. The maximum swept-path width is 8.70 m when the minimum curve radius is 12.5 m. As the curve radius increases, the maximum swept-path width decreases, and the decreasing slope is steeper while the curve radius is smaller than 25m. When the curve radius is 50m, the maximum swept-path width becomes 3.91m.

Since the amount of offtracking is the difference in the paths of the front and rear wheels of the vehicle, it describes the additional width the vehicle occupies to negotiate a turn. Therefore, it is also the amount by which a turning roadway must be widened. As Fig. 16 shows, maximum offtracking is 2.36 times the width of semitrailer when the curve radius is 12.5m, and decreases to 1.08 and 0.51 times when the radius equals 25m and 50m, respectively.

The offtracking of the roadway section after the turn converges more slowly. For example, for a roadway with a 12.5 m radius, a tangent section of 23.68 m (after point of curve to tangent, PT) is needed to reduce offtracking to 0.5m. On highway and street engineering design, a minimum clearance of 0.5 m should be provided for the curb face and other obstructions [2]. Reducing offtracking to 0.2 m (about the width of a tire) requires a tangent section of 33.53 m.

The composition of a vehicle turning path includes the paths of the outer front wheel and inner rear wheel. The path of the outer front wheel is approximately the offset curve of the centerline of the roadway alignment. However, the path of inner rear wheel is more complex. For turning roadway sections where the swept-path width remains constant, the path of the inner rear wheel describes an arc concentric with the circular alignment. This study also considers turning roadway sections where the swept-path width is still changing, and finds that the paths of the inner rear wheel could not be adequately described as clothoid curves or polynomial curves. In engineering design practice, three-centered compound curves are sometimes adopted in right-turn roadways to design the inner edges of curbs. The computational approach can help to increase precision in designing roadway configurations.

### Steering Angle

Figs. 17 and 18 show the curves of simulated steering and articulating angles for roadways with different radii. All the steering angle curves yield to a stable maximum value after entering the circular curve for a certain distance. The roadways which have a radius greater than 25m could also reach stable maximum articulating angles. Fig. 19 shows the effects of curve radius on maximum steering and articulating angles ( $Max.\theta_s / Max.\theta_a$ ).

The steering angle directly relates to the turning angle of the steering wheel, and therefore the curves of the steering angle can be used to evaluate the steering motion. As shown in Fig. 17, roadways with smaller radii require greater rotation of the steering wheel. The articulating angle is the deflection angle of the vehicle body. When the articulating angles are greater or changing, drivers of

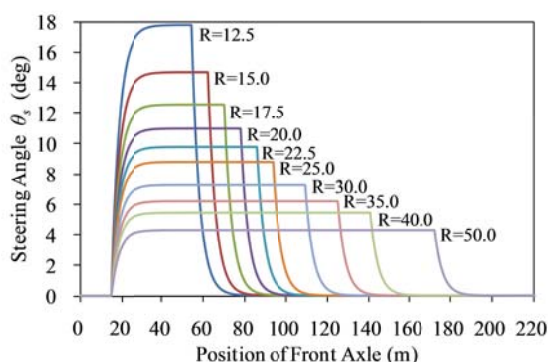


Fig. 17. Steering Angles of Different Radius Roadways.

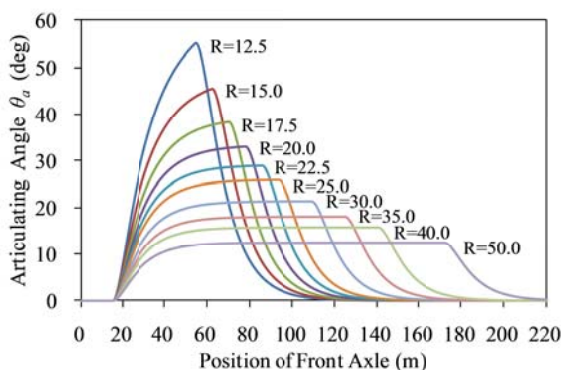


Fig. 18. Articulating Angles of Different Radius Roadways.

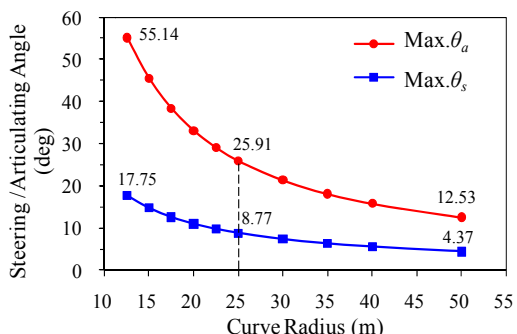


Fig. 19. Effect of Curve Radius on Max. Steering/Articulating Angles.

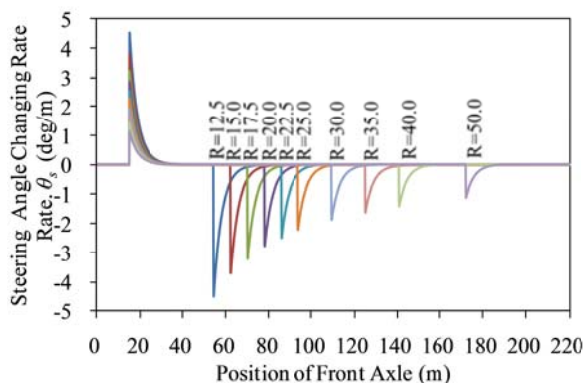


Fig. 20. Steering Angle Changing Rates of Different Radius Roadways.

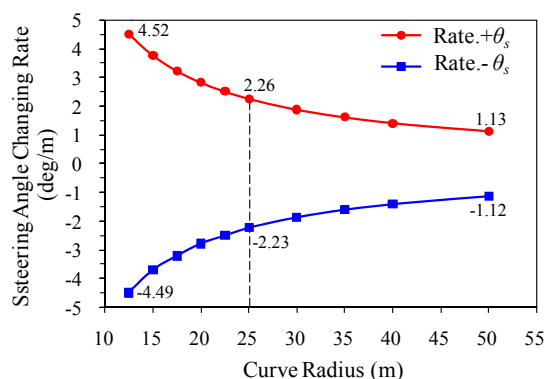


Fig. 21. Effect of Curve Radius on Max. Steering Angle Changing Rate.

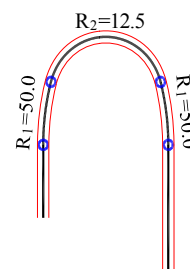


Fig. 22. Roadway with Compound Curve.

combination trucks need to pay more attention and repeatedly look back toward the vehicle body.

Fig. 20 shows the curves of steering angle changing rates for roadways with different radii, while Fig. 21 shows the effect of curve radius on maximum steering angle changing rate. The changing rates of the steering angle are related to the angular speed of steering wheel. Due to the discontinuous curvature of roadway alignment, each curve in Fig. 20 has two peaks at the entering and leaving sections, respectively. The peak values of the steering angle changing rates increase as the curve radius decreases (Fig. 21).

Field experiments demonstrate that when drivers could not successfully respond to the change in peak, they would make the transition themselves to reduce the impact of discontinuous curvature. This un-designed transition in driving behavior would result in the turning vehicle driving slightly off the roadway alignment. The curves of steering angles, their changing rates, and the curves of articulating angles could be integrated to analyze the ease and smoothness of driving operations.

### Compound Curve

Compound curves are commonly applied in designs for turning roadways or the edges of traveled ways. Since the curve radii have significant effects on the peak values of the rate of change for steering angles, this study simulated a roadway alignment with a compound curve to examine its effect on turning operations. The roadway alignment consists of three circular curves (with radii of 50, 12.5, and 50 m) and tangent sections with a 180° turning angle (Fig. 22).

Fig. 23 shows the steering and articulating angles of compound-curve roadways. The maximum steering angle and maximum articulating angle are almost the same with simple-curve

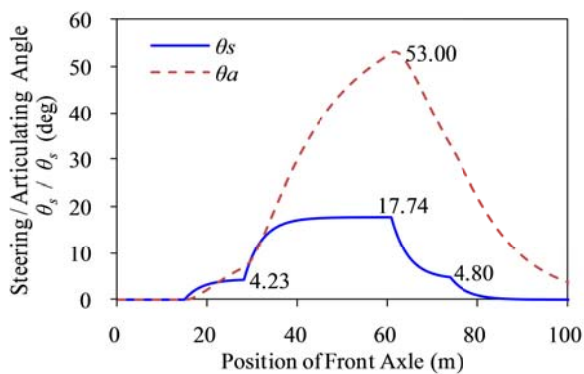


Fig. 23. Steering/Articulating Angles of Compound Curve

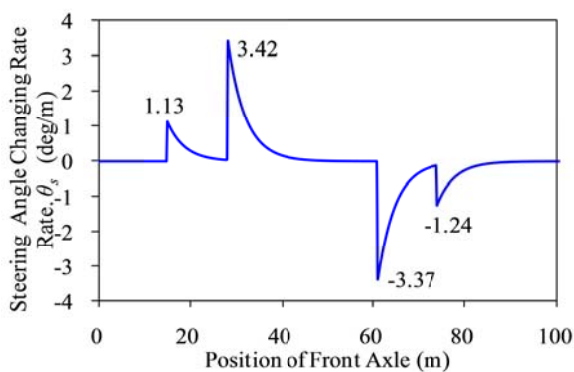


Fig. 24. Steering Angle Changing Rate of Compound Curve

roadway. Fig. 24 shows the steering-angle changing rates. The compound-curve roadway alignment does reduce the peak values, but more peaks appear at points where curvature is discontinuous.

Roadway geometric design should be compatible with the capabilities and limitations of drivers, and help reduce driver error by avoiding complex design features. The compound-curve roadway alignment could result in frequent changes of steering angular speed and unsteady steering behavior, and thus counteract its effect on the reduction of the peak values of steering angle changing rate. Analysis of steering operations suggests that compound curves are not suitable for the design of turning roadway alignments.

## Conclusion

This study examines the effects of roadway geometric features on low-speed vehicle turning maneuvers, which mainly includes vehicle turning paths and driving operations. Specifically, this study presents a computational approach to calculate the vehicle turning paths of roadways with different geometric characteristics. The proposed approach can also evaluate driving operations by simulating variations of steering and articulating angles. The computational method was first used to check for coincidence with design standards. Field experiments using large vehicles on roadways with different turning angles and geometric features were conducted. Turning paths of wheels and operations of steering wheel were recorded. The results of field experiments were compared with those of the computational method, and effects of curve radius and geometric features on turning maneuver were then analyzed. Precise analyses of vehicle turning maneuvers, including

turning paths, swept widths and driving operations could benefit roadway and pavement engineering design application to improve traffic safety and efficiency.

## References

- MOTC (2008). Design Specification for highway alignment, Ministry of Transportation and Communications, Taiwan (in Chinese).
- AASHTO (2004). A Policy on Geometric Design of Highways and Streets, 5th Edition, American Association of State Highway and Transportation Officials, Washington, DC, USA.
- Millar, D.S. and Walton, C.M. (1985). Offtracking of the Larger Combination Commercial Vehicles, *Transportation Research Record*, No. 1026, pp. 62-65.
- SAE (1998). Turning Ability and Off Tracking—Motor Vehicles, Surface Vehicle Recommended Practice J695 DEC89, Society of Automotive Engineers, Warrendale, PA, USA.
- WHI (1970). Offtracking Characteristics of Trucks and Truck Combinations, Research Committee Report No. 3, Western Highway Institute, San Francisco, California, USA.
- Sayers, M. (1984). FHWA/UMTRI Vehicle Offtracking Model and Computer Simulation—User's Guide, Version 1.0, University of Michigan Transportation Research Institute, Ann Arbor, Michigan, USA.
- Fong, K.T. and Chenu, D.C. (1986). Simulation of Truck Turns With a Computer Model, *Transportation Research Record*, No. 1100, pp. 20-29.
- CalTran (1985). Truck Offtracking Model (TOM), Program Documentation and User's Guide, Division of Transportation Planning, California Department of Transportation, USA.
- Analysis Group (1986). FHWA Vehicle Offtracking Model—IBM PC Version 1.0: Program Documentation and User's Guide, FHWA, US Department of Transportation, Washington, DC, USA.
- Transoft Solutions (2010). AutoTURN User's Guide, Richmond, British Columbia, Canada.
- Carrasco, M.S.E. (1995). Turning Vehicle Simulation: Interactive Computer-Aided Design and Drafting Application, *Transportation Research Record*, No. 1500, pp. 1-11.
- Savoy Computing (2010). User Manual for AutoTrack, Kent, England.
- Freedman, H.I. and Riemenschneider, S.D. (1983). Determining the Path of the Rear Wheels of a Bus, *SIAM Review*, 25(4), pp. 561-567.
- Alexander, J.C. and Maddocks, J.H. (1988). On the Maneuvering of Vehicles, *SIAM Journal on Applied Mathematics*, 48(1), pp. 38-51.
- Wang, Y. and Linnett, J.A. (1995). Vehicle Kinematics and its Application to Highway Design, *ASCE Journal of Transportation Engineering*, 121(1), pp. 63-74.
- Prince, G.E. and Dubois, S.P. (2009). Mathematical Models for Motion of the Rear Ends of Vehicles, *Mathematical and Computer Modelling*, 49(9-10), pp. 2049-2060.
- Wang, Y. and Cai, K. (1999). On a Driving Hazard Problem, *The Mathematical Gazette*, 83(497), pp. 226-236.
- Gattis, J.L. and Howard, M. D. (1999). School Bus Design

- Vehicle Dimensions, *Transportation Research Record*, No. 1658, pp. 70-76.
19. Terry, P. A. and Schuster, J. J. (1996). Tractor-trailer reverse movement path, *ITE Journal*, 66(11), pp. 38-43.
  20. Smith, W.S. (2003). *Moving Average Filters, Digital Signal Processing: a Practical Guide for Engineers and Scientists*, pp. 277-284, Elsevier Science, Burlington, MA, USA.
  21. Pacejka, H.B. (2006). *Tyre Characteristics and Vehicle Handling and Stability, Tyre and vehicle dynamics*, 2nd Edition, pp. 10, Elsevier Science, Burlington, MA, USA.